

# Dual Scale-aware Adaptive Masked Knowledge Distillation for Object Detection

1<sup>st</sup> ZhouRui Zhang

*school of computing*

*Nanjing Normal University*

Nanjing, Jiangsu

222212067@njnu.edu.cn

2<sup>st</sup> Jun Li\*

*school of computing*

*Nanjing Normal University*

Nanjing, Jiangsu

lijunest@njnu.edu.cn

3<sup>rd</sup> JiaYan Li

*school of computing*

*Nanjing Normal University*

Nanjing, Jiangsu

232212021@njnu.edu.cn

4<sup>th</sup> ZhiJian Wu

*School of Data Science and Engineering*

*East China Normal University*

City, Country

zjwu\_97@stu.ecnu.edu.cn

5<sup>th</sup> JianHua Xu

*school of computing*

*Nanjing Normal University*

Nanjing, Jiangsu

xujianhua@njnu.edu.cn

**Abstract**—Recent feature masking knowledge distillation methods make use of attention mechanisms to identify either important spatial regions or channel clues for discriminative feature reconstruction. However, most of existing strategies perform global attention-guided feature masking distillation without delving into fine-grained visual clues in feature maps. In particular, uncovering locality-aware clues across different scales are conducive to reconstructing region-aware features, thereby significantly benefiting distillation performance. In this study, we propose a fine-grained adaptive feature masking distillation framework for accurate object detection. Different from previous methods in which global masking is performed on single-scale feature maps, we explore the scale-aware feature masking by performing feature distillation across various scales, such that the object-aware locality is encoded for improved feature reconstruction. In addition, our fine-grained feature distillation strategy is combined with a masking logits distillation scheme in which logits difference between teacher and student networks is utilized to guide the distillation process. Thus, it can help the student model to better learn from the teacher counterpart with improved knowledge transfer. Extensive experiments for detection task demonstrate the superiority of our method. For example, when RetinaNet, RepPoints and Cascade Mask RCNN are used as teacher detectors, the student network achieves mAP scores of 41.5%, 42.9%, and 42.6%, respectively, outperforming state-of-the-art methods such as DMKD and FreeKD.

**Index Terms**—Feature Masking Knowledge Distillation, Scale-aware Feature Masking, Masking Logits Distillation, Object Detection

## I. INTRODUCTION

Knowledge distillation (KD) is capable of improving the performance of a small model (student) with the help of a larger network (teacher) via effective knowledge transfer. It allows the deployment of the student model in resource-constrained scenarios with lower computational budgets. Known as logit distillation (LD), numerous LD methods function by aligning the logits between dual networks, such that the student can directly learn from the teacher model for accurate classification. In addition, another major line of research in

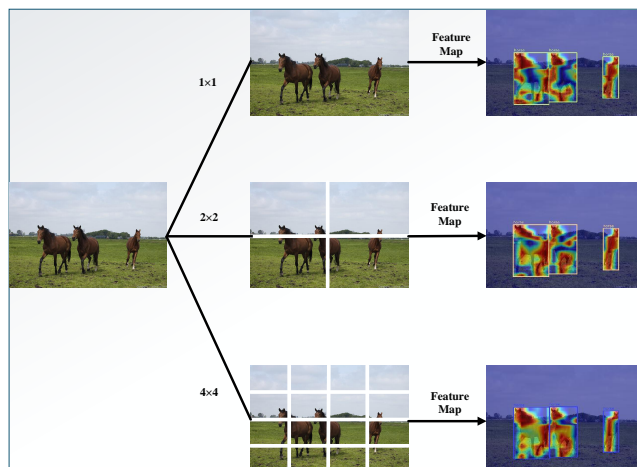


Fig. 1. By dividing the images into 1×1, 2×2, and 4×4 segments, and then training the RetinaNet model on each segmented image to obtain feature maps, the generated multi-scale heatmaps after merging show noticeable differences. We observe that the model focuses on different regions for images of varying sizes. The larger the segmentation size, the more attention the model pays to the target details in the image, leading to better differentiation between foreground and background.

KD methods is feature distillation (FD) which helps the student to generate discriminating representations by imitating the teacher feature maps. Different from conventional FD methods, recent feature masking distillation schemes replace “feature imitation” with “feature reconstruction”. Taking advantage of masking mechanism, discriminative feature encoding can be reconstructed from the selectively masking regions of the student feature maps, which significantly boosts the feature learning capability of the student model. In particular, attention-guided masking strategies help to exploring abundant semantic-aware clues, and thus tremendously promotes the FD performance in a variety of downstream tasks including object classification and detection.

\*Corresponding author

In object detection, imbalance between foreground and background regions poses great challenges to detection accuracy, since the background pixels in an image usually outnumber the foreground counterparts. Thus, some important clues are likely to be downplayed especially when the student network typically mimics the features built on all the image pixels without ade

The final layer of object detection usually integrates feature information from the entire image to make the final decisions about the categories and locations of objects. Although feature-based distillation can transfer feature information, it does not ensure consistency in category prediction and localization. Therefore, introducing logit-based distillation is necessary. However, similar to feature extraction, distilling the entire logit might compromise overall distillation performance.

To address the issues mentioned above, we propose the DSAMD method. Specifically, DSAMD divides the global feature maps into multiple local feature maps and utilize the feature masking mechanism guided by spatial differences, enabling the model to focus more effectively on the critical regions within each feature map. This facilitates the student’s learning of local features and boundary details, allowing the model to better distinguish between foreground and background. Furthermore, we employ feature-level masks as guidance to assist logit in locating informative regions. The contributions of our work are as follows:

- We observed that the model’s attention to the edge details of target objects varies across different scales. Therefore, we propose DSAMD Framework, including Scale-aware Feature Maps(SA module) and Adaptive Masked Weights(AM module), which enhances the model’s learning of local features and boundary information, thereby enabling better distinction between foreground and background.
- We integrate feature-based distillation and logit-based distillation by utilizing feature-level masks as guidance to assist logit in locating information more effectively.
- Extensive experiments on detection tasks demonstrate the promising performance of our method in knowledge distillation for object detection.

## II. RELATED WORK

### A. Knowledge Distillation

In recent years, dramatic progress has been made in knowledge distillation, and we will comprehensively review different approaches to knowledge distillation. Existing work can be broadly classified into two categories: feature-based methods and logitbased methods.

Feature-based methods primarily extract knowledge from intermediate feature layers. Tang et al. [13] ingeniously designed distillation weights and loss functions to enable automatic adjustment based on samples in single-stage object detectors. Yang et al. [11]introduced FGD, which separates the foreground and background, allowing the student model to learn from the key regions and global knowledge of the

teacher network through focal and global distillation respectively. Yang et al. [14] proposed prediction-guided distillation, focusing on distilling the key prediction regions of the teacher. Cao et al. [15]proposed PKD distillation, which uses Pearson correlation coefficients to mimic features, focusing on relational information from the teacher while relaxing the constraints on feature size. Zheng et al. [16] transferred knowledge distillation from the classification head to the localization head in object detection and proposed a new distillation mechanism called LD, revealing that knowledge of object categories and object locations should be handled separately.

Logit-based methods primarily extract knowledge from logit and transfer it to the student model. Zhao et al. [17] proposed DKD, which reformulates the classical KD loss into two parts, i.e. target class knowledge distillation and non-target class knowledge distillation, thereby considering the importance of each part separately. Lee et al. [18] proposed QMKD, which uses reinforcement learning to extract latent information from both teachers and students, thereby enhancing the knowledge distillation process.

### B. Object Detection

Object detection is a key task in the field of computer vision, aiming to identify and localize specific objects within images. It is widely recognized that current deep model-based object detection methods can generally be categorized into three types: anchor-based detectors [19], anchor-free detectors [20]–[22], and end-to-end detectors [23]. Anchor-based detectors include single-stage, which offer faster speeds by directly generating bounding boxes and class info, and two-stage, which achieve higher accuracy using RPN and RCNN heads but are slower. Anchor-free methods, like CornerNet and CenterNet, bypass anchor box design and rely on local perception for object prediction. With the rise of the Transformer architecture, advanced end-to-end Transformer-based detectors such as DETR [24] and Deformable DETR [25] have achieved remarkable success in recent years. These methods enable models to better capture global contextual information within images and reduce the need for manually designed components. However, this also significantly increases the computational resources and costs required.

## III. METHODS

First, I list the main symbols used in this section to simplify the presentation. We denote the features of each FPN layer as  $F \in R^{H \times W \times C}$ , and the logit (scores generated in the classification head) as  $L \in R^{H \times W \times K}$ , where H, W, C, and K represent height, width, channels, and the number of classes, respectively. The corresponding losses are denoted as  $L_{feat}$  and  $L_{logit}$ . We distinguish between F and L based on the superscripts S and T for the student and teacher, respectively.

Before providing a detailed introduction to the method we propose, we briefly review feature-based distillation frameworks, feature-mask-based distillation frameworks, and logit-based distillation frameworks. The formula as follows:

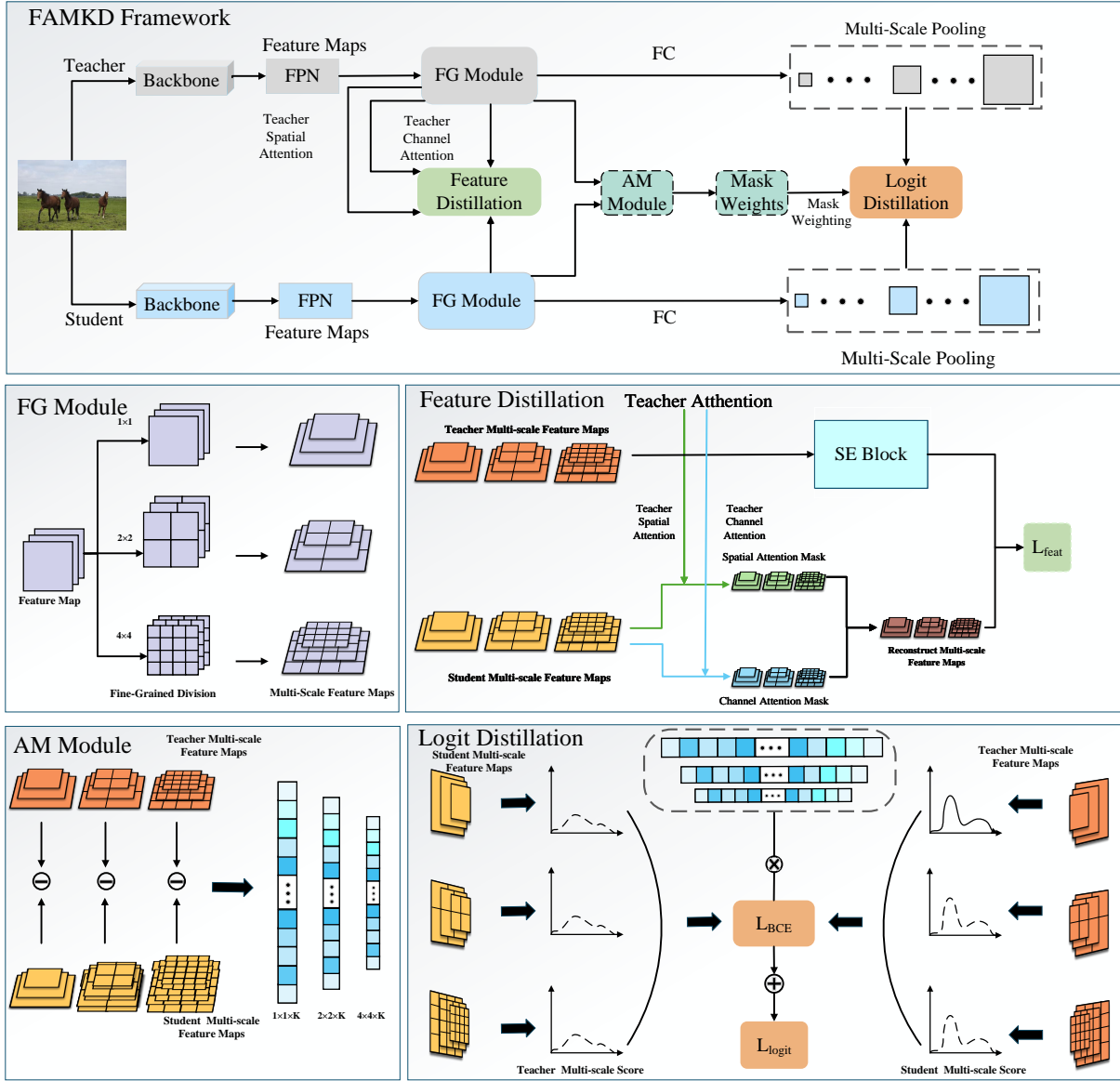


Fig. 2. Our proposed DSAMD distillation framework. First, through the SA module, we perform multi-scale pooling to allow the model to focus on key features in different regions of the input image. At each scale, spatial and channel attention propagation is established, enabling the student network to learn edge and global information through attention mechanisms at different scales, and reconstruct feature maps across various scales. Next is the AM module, We were prompted to pass the difference between the feature maps of teachers and students as auxiliary mask information to the logit layer at the feature level, guiding the student's final layer student's final layer's output.

$$F_{NEW}^S = \theta_S(M_S \cdot F_S^S) + \theta_C(M_C \cdot F_C^S) \quad (1)$$

$$L_{FeatureMask}^{original} = \sum(A(F_{NEW}^S, F^T)) \quad (2)$$

In this equation, the subscript  $S/C$  denotes the spatial and channel dimensions, respectively.  $M_S$  and  $M_C$  represent the spatial and channel masks generated through the teacher's spatial and channel attention, while  $\theta$  is the feature reconstruction function. The traditional logit-based distillation framework predicts the corresponding results through the scores generated

by the classification head in the final layer. The formula is as follows:

$$L_{logit}^{original} = \sum(D(L^S, L^T)) \quad (3)$$

Here,  $D(\cdot)$  represents the commonly used loss functions for logit distillation, such as  $KL$  or  $BCE$ .  $L^{S/T} \in R^{H \times W \times K}$  is the score map generated by the classification head of the final layer from the student or teacher network.

Although the aforementioned dual-mask feature extraction scheme can reconstruct student features with enhanced representational ability, it does not focus on the target's detailed

parts, especially at the foreground-background boundary. The dual-mask feature extraction scheme enhances representation but overlooks important boundary details. To address this, we propose DSAMD, which improves edge detail learning by combining feature and logit distillation. As shown in Fig. 2, based on DMKD [26], fine-grained division refines detail focus, and use the difference(Cosine distance) between the teacher and student feature maps as a spatial mask weight to optimize the multi-scale score map, boosting performance. DSAMD efficiently transmits precise information through refined control over Fine-grained details.

#### A. SA Moudle

This section details the proposed SA (Fig. 2), where multi-scale pooling performs max-pooling at different scales on the teacher’s and student’s feature maps (F T and F S) to emphasize key features across regions. Unlike average pooling, which is less effective for feature distillation, this approach retains more semantically precise fine-grained knowledge, offering advantages over traditional global feature-based KD.

Next, we propagate spatial and channel attention through the teacher’s feature maps at different scales. The student network learns edge and global details via attention mechanisms and reconstructs feature maps at multiple scales. The local feature maps are weighted and combined with the global map. SA guides the student to focus on blurred edge details where local and global categories conflict.

Specifically, multi-scale pooling splits the feature map into units of different scales and performs a max-pooling operation to aggregate the feature information within each unit. Let  $S(x, y)$  represent the spatial map of the  $x$ -th unit at the  $y$ -th scale, and  $M(x, y)$  represent the feature region corresponding to this unit.  $I_{T/S}(x, y) \in R^{C \times 1 \times 1}$  denotes the feature layer information of the region  $M(x, y)$  from the teacher or student, which is the feature map that aggregates the feature knowledge of this unit. The formula is as follows:

$$I_T(x, y) = \sum_{(h,w) \in S(x,y)} \text{MAX} [F_T(h, w)] \quad (4)$$

$$I_S(x, y) = \sum_{(h,w) \in S(x,y)} \text{MAX} [F_S(h, w)] \quad (5)$$

Here,  $(h, w)$  represents the height and width of the feature map in  $S(x, y)$ , where  $h, w \in S(x, y)$ .  $C$  is the number of channels in the original feature map, which varies with the size changes.  $F_T$  and  $F_S$  are the feature maps of the teacher and student at the original size, respectively, and the  $x$  and  $y$  coordinates of the teacher and student are correspondingly aligned.

After Fine-grained division refinement, the teacher transmits spatial and channel attention to the student, who learns the masks and reconstructs feature maps to the corresponding size. These maps also provide weight information for logit distillation. Finally, both teacher and student feature maps are interpolated back to the original size to prevent semantic misalignment and ensure consistent knowledge learning for

the regions. First, the spatial and channel attention maps are generated based on the teacher’s features, as shown in the following formula:

$$A_s(x, y) = \phi(\text{Sigmoid}(\frac{1}{C\tau} \sum_{n=1}^N \|I_{T_n}(x, y)\|_2^2)) \quad (6)$$

$$A_c(x, y) = \text{Sigmoid}(\frac{1}{HW\tau} \sum_{c=1}^C \sum_{(h,w)} I_{T_{h,w,c}}(x, y)) \quad (7)$$

Where  $\phi$  is the spatial mapping function,  $A_s$  and  $A_c$  are the spatial and channel attention maps at different scales, and  $x$  and  $y$  represent the unit and scale, respectively. In Eq.(6),  $I_{T_n}$  is the  $n$ -th vector of the teacher’s feature map at different scales, while in Eq.(7),  $I_{T_{h,w,c}}$  represents the feature map of the  $c$ -th channel at different scales. The parameter  $\tau$  is introduced to adjust the distribution [reference]. Next, the obtained spatial and channel attention maps  $A_s$  and  $A_c$  are used to derive the corresponding mask maps  $M_s$  and  $M_c$ , classified by the thresholds  $\omega_s$  and  $\omega_c$ , as shown in the following formula:

$$M_{s_{(i,j) \in S(x,y)}}(x, y) = \begin{cases} 0 & A_{s_{i,j}}(x, y) \geq \omega_{s_{i,j}}(x, y) \\ 1 & \text{Otherwise} \end{cases} \quad (8)$$

$$M_{c_{t \in C}}(x, y) = \begin{cases} 0 & A_{c_t}(x, y) \geq \omega_{c_t}(x, y) \\ 1 & \text{Otherwise} \end{cases} \quad (9)$$

Where  $x$  and  $y$  are the same as previously mentioned, and  $M_s$  and  $M_c$  at each scale have the same shape as the corresponding  $A_s$  and  $A_c$  at that scale. Then, we use these masks to apply spatial and channel masking on the student’s feature map  $I_S$  at different scales, generating the masked feature maps  $F_s^S$  and  $F_c^S$  at each scale, as shown in the following formula:

$$F_s^S(x, y) = \Theta(I_S(x, y)) \otimes M_s(x, y) \quad (10)$$

$$F_c^S(x, y) = \Theta(I_S(x, y)) \otimes M_c(x, y) \quad (11)$$

Where  $\Theta$  represents the feature mapping, and  $\otimes$  denotes element-wise multiplication. Finally, two different reconstruction blocks, based on convolution and perceptron, are used to reconstruct the masked features in the spatial and channel directions. After obtaining the reconstructed feature maps at each size, they are interpolated back to the feature map of the original size, resulting in the final student features, as shown in the following formula:

$$F_{rec}^S(x, y) = \lambda \cdot \theta_s(F_s^S(x, y)) + \mu \cdot \theta_c(F_c^S(x, y)) \quad (12)$$

$$F_{new}^{S_{y=1,2,4}} = IP(F_{rec}^S(x, y), (H, W)) \quad (13)$$

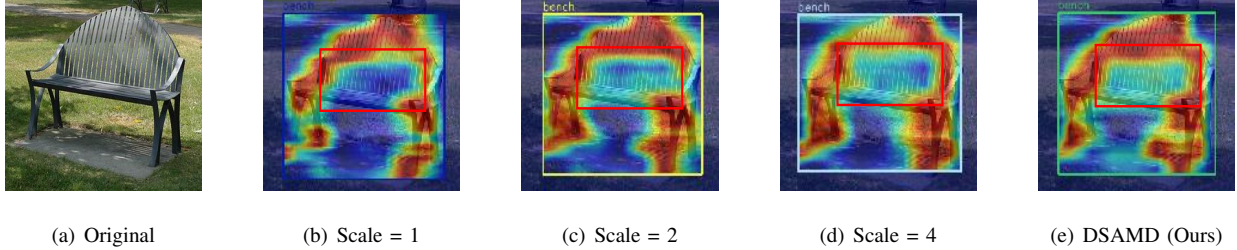


Fig. 3. Here are the visualizations of the feature maps obtained from the training of our SA module. (a) is the original image, (b), (c), and (d) show the results obtained by training with three different scales individually, while (e) represents the Fine-grained division method combining all three scales. It is evident that the Fine-grained division approach extracts more target features. The teacher detector is Retinanet-ResNeXt101, and the student detector is Retinanet-ResNet50.

Here,  $\lambda$  and  $\mu$  are the adjustment weighting factors,  $\theta_s$  and  $\theta_c$  represent the convolution and perceptron reconstruction blocks, respectively, and  $IP(\cdot)$  is the interpolation function.  $y$  denotes different scales, and  $(H, W)$  refers to the original size, which is the same as the shape of the original teacher feature map. In our experiments, three scales are ultimately selected: 1, 2, and 4. Therefore, the feature distillation loss can be established by weighted summation of the final student features  $F_{new}^S$  and the corresponding teacher features  $F^T$  at these three scales.

We observed that when using all three scales simultaneously, our DSAMD achieves significant mAP improvements, demonstrating the effectiveness of the proposed method. We also provide visualizations of the feature maps obtained at different scales, as shown in Fig. 3. It is evident that the object features generated by our DSAMD are more distinguishable than those generated at a single scale.

### B. AM Mouldle

Next, we will describe the proposed AM (Fig. 2). First, we extract feature maps of students and teachers at each scale, and calculate the difference between them as spatial mask weights to assist in logit distillation. AM highlights the pixel-level gap between the student and teacher. By passing this spatial mask to the logit layer, we can better guide students' final output, enhance the score map of the target area, and thus better narrow the overall gap between students and teachers.

Specifically, to align with the teacher's masks at different scales, we apply pooling operations on the final layer, with average pooling used for fine-grained operations to capture global information. This prevents background scores from affecting the effectiveness of multi-scale pooling. Let  $S_f(x, y)$  represent the spatial region of the  $x$ -th unit at the  $y$ -th scale, and  $M_f(x, y)$  represent the corresponding input region.  $Z(x, y) \in R^{K \times 1 \times 1}$  denotes the logit output score map of the teacher for the region  $M_f(x, y)$ , which is the aggregated logit knowledge of this unit. The formula is as follows:

$$Z_T(x, y) = \sum_{(p,q) \in S_f(x,y)} \frac{L_T(p, q)}{x^2} \quad (14)$$

$$Z_S(x, y) = \sum_{(p,q) \in S_f(x,y)} \frac{L_S(p, q)}{x^2} \quad (15)$$

Where  $(x, y)$  is as previously mentioned, and  $(p, q)$  denotes the coordinates of the logit output in  $S_f(m, n)$ . Here, we choose average pooling for scale refinement in order to preserve global feature information. By utilizing the teacher's attention mask, we expand the local feature information. The formula is as follows:

$$M_{s,a,b}^{weights}(x, y) = SIM(I_{T_{a,b}}(x, y), I_{S_{a,b}}(x, y)) \quad (16)$$

Where  $(a, b)$  represents the spatial index, and  $I_{S/T}(x, y)$  is as previously mentioned. We assume that  $SIM(\cdot)$  is equivalent to  $\cos(u, v) = 1 - \frac{u^T v}{\|u\|_2 \|v\|_2} \in [0, 2]$ . Therefore, the logit distillation loss can be established by weighted summation of the final score maps  $Z_{S/T}(x, y)$  for the teacher and student at three different scales, with the assistance of  $M_{s,a,b}^{weights}(x, y)$ .

### C. Loss Function

The overall loss function used to train DSAMD can be expressed as:

$$L_{DSAMD} = \alpha L_{Feat} + \beta L_{Logit} + L_{Det} \quad (17)$$

Where  $L_{Det}$  is the original detection loss, and  $L_{Feat}$  and  $L_{Logit}$  represent the feature distillation loss and logit distillation loss, respectively, as shown below:

$$L_{Feat} = \sum_{y=1,2,4} \sum_{c=1}^C \sum_{h=1}^H \sum_{w=1}^W (F_{c,h,w}^{T_y} - \Theta(F_{new}^{S_y}))^2 \quad (18)$$

$$L_{Logit} = \sum_{x,y} \sum_{h,w=1,1}^{H,W} M_s^w(x, y) \cdot D(Z_T(x, y), Z_S(x, y)) \quad (19)$$

Where  $C$ ,  $H$ , and  $W$  represent the number of channels, height, and width of the feature map, respectively;  $x$  and  $y$  represent the number of units and the scale at that scale, with  $x \in [1, N]$ .  $D(\cdot)$  is the logit distillation loss function, either  $KL$  or  $BCE$  loss. Experiments have shown that using the  $KL$  loss function yields better results. In the above equation,  $\alpha$  and  $\beta$  are hyperparameters that balance the different terms.

TABLE I  
COMPARISON OF OUR METHOD WITH OTHER DISTILLATION METHODS FOR OBJECTION ON COCO

Teacher	Student	mAP	APs	APm	API	mAR	ARs	ARm	ARI
RetinaNet ResNeXt101	RetinaNet-Res50	37.4	20.6	40.7	49.7	53.9	33.1	57.7	70.2
	FKD	39.6(+2.2)	22.7	43.4	52.5	56.1(+2.2)	36.8	60.0	72.1
	FGD	40.7(+3.3)	22.9	45.0	54.7	56.8(+2.9)	36.5	61.4	72.8
	DiffKD	40.7(+3.3)	22.2	45.0	55.2	56.9(+3.0)	36.4	61.6	72.8
	MGD	41.0(+3.6)	23.4	45.3	55.7	57.0(+3.1)	37.2	61.7	72.8
	FreeKD	41.0(+3.6)	22.3	45.1	55.7	57.1(+3.2)	37.3	61.7	72.9
	DMKD	41.3(+3.8)	<b>23.5</b>	45.4	55.2	57.6(+3.7)	<b>37.4</b>	<b>62.0</b>	73.2
<b>DSAMD(Ours)</b>	<b>41.6(+4.1)</b>	<b>23.5</b>	<b>45.6</b>	<b>55.8</b>	<b>57.7(+3.8)</b>	37.2	<b>62.0</b>	<b>73.7</b>	
RepPoints ResNeXt101	RepPoints-Res50	38.6	22.5	42.2	50.4	55.1	34.9	59.4	70.3
	FKD	40.6(+2.0)	23.4	44.6	53.0	56.9(+1.8)	37.3	60.9	71.4
	FGD	42.0(+3.4)	24.0	45.7	55.6	58.2(+3.1)	37.8	62.2	73.3
	DiffKD	41.7(+3.1)	23.6	45.4	55.9	58.1(+3.0)	37.9	62.0	73.1
	MGD	42.3(+3.7)	24.4	46.2	55.9	58.4(+3.3)	40.4	62.3	73.9
	FreeKD	42.4(+3.8)	24.3	46.4	<b>56.6</b>	58.6(+3.5)	40.4	62.4	74.0
	DMKD	42.6(+4.0)	24.6	46.6	56.2	58.8(+3.7)	40.5	62.4	74.2
<b>DSAMD(Ours)</b>	<b>42.9(+4.3)</b>	<b>25.0</b>	<b>46.8</b>	56.3	<b>59.0(+3.9)</b>	<b>40.7</b>	<b>62.6</b>	<b>74.3</b>	
Cascade Mask RCNN ResNeXt101	Faster RCNN-Res50	38.4	21.5	42.1	50.3	52.0	32.6	55.8	66.1
	FKD	41.5(+3.1)	23.5	45.0	55.3	54.4(+2.4)	34.0	58.2	69.9
	FGD	42.0(+3.6)	23.8	46.4	55.5	55.4(+3.4)	<b>35.5</b>	60.0	70.0
	DiffKD	42.2(+3.8)	24.2	46.6	55.3	55.5(+3.5)	<b>35.5</b>	60.1	70.7
	MGD	42.1(+3.7)	23.7	46.4	56.1	55.5(+3.5)	35.4	60.0	70.5
	FreeKD	42.4(+4.0)	24.1	<b>46.7</b>	55.9	55.8(+3.8)	35.4	60.0	70.6
	DMKD	42.4(+4.0)	24.1	46.5	56.2	55.8(+3.8)	35.3	60.0	70.7
<b>DSAMD(Ours)</b>	<b>42.6(+4.2)</b>	<b>24.2</b>	46.6	<b>56.4</b>	<b>55.9(+3.9)</b>	<b>35.5</b>	<b>60.2</b>	<b>70.9</b>	

#### IV. EXPERIMENTS

##### A. Experimental Setup

We evaluated our knowledge distillation method on COCO dataset [27], which comprises over 320k images of 80 different object categories with abundant annotations. We use the 120k train images for training and 5k val images for testing for all the experiments. Within our experiments, including RetinaNet [9], Cascade Mask R-CNN [2], Faster R-CNN [28], RepPoints [21]. For performance measure, we follow [29] to adopt Average Precision (AP) and Average Recall (AR) as metrics. All the experiments are conducted on a desktop with an Intel(R) Core(TM) i9-10900K CPU and a 3090 GPU under the PyTorch framework. During the training process, SGD optimizer is used for training all the detectors within 24 epochs. Meanwhile, momentum is set as 0.9 whilst weight decay is set to 0.0001. To demonstrate the superiority of our DSAMD model, numerous state-of-art(SOTA) methods are involved in our comparative studies, including FGD [11], FKD [30], DiffKD [31], MGD [32], DMKD [26], FreeKD [33].

##### B. Results

In our comparative studies, we carry out three groups of experiments to evaluate different distillation methods with the three popular detectors involved. The corresponding experimental results are shown in Table I.

TABLE II  
ABLATION STUDIES USING RETINANET FRAMEWORK FOR BOTH THE TEACHER AND THE STUDENT. SA AND AM ARE THE MAIN COMPONENTS OF OUR PROPOSED DSAMD MODEL.

Teacher: <i>RetinaNet-ResNeXt101</i>		
Student: <i>RetinaNet-Res50</i>		
SA	AM	mAP
✓		41.5
	✓	41.4
✓	✓	<b>41.6</b>

TABLE III  
COMPARISON OF DIFFERENT POOLING STRATEGIES FOR FINE-GRAINED DIVISION METHOD

<i>Mutli-Scale Method</i>	<i>Avg Pooling</i>	<i>Max Pooling</i>
mAP(%)	41.2	<b>41.5</b>

TABLE IV  
THE IMPACT OF MASK WEIGHTING ON LOGIT METHOD

<i>logit Method</i>	<i>Original</i>	<i>Mask Weighting</i>
mAP(%)	41.3	<b>41.4</b>



TABLE V  
PERFORMANCE OF THE DSAMD AT DIFFERENT SCALES.

<i>Teacher: RetinaNet-ResNeXt101</i>			
<i>Student: RetinaNet-Res50</i>			
Scale = 1	Scale = 2	Scale = 4	mAP
✓			41.3
	✓		41.3
		✓	41.4
✓	✓		41.3
✓		✓	41.4
	✓	✓	41.5
✓	✓	✓	<b>41.6</b>

In the first group of experiments, we employed RetinaNet as the detection framework for both the teacher and student. The experimental results show that our proposed method achieves a notable performance improvement of 4.1% in mAP compared to the baseline student network, reaching an accuracy of 41.6%. This result consistently outperforms SOTA methods such as FreeKD and DMKD by 0.5% and 0.3%, respectively. Similar enhancements are observed in the mAR metric, further demonstrating the effectiveness of our approach. The experimental setup in the second group mirrors that of the first group, with the key difference being the substitution of the RetinaNet framework with RepPoints. In line with the results from the first group, we observed significant improvements of 4.3% in mAP and 3.9% in mAR, and similar performance superiority to the competing distillation methods is also demonstrated. These results suggest that our approach enables the student model to effectively extract and utilize more critical information from the teacher, leading to substantial performance boosts and significant contributions to the overall improvement of the student model.

To further evaluate the generalization of our method, we use different detection frameworks for the teacher and student models, employing stronger backbone-based teacher detectors. To be specific, the more powerful detector Cascade Mask-RCNN is used as the teacher network while the Faster-RCNN for the student model. As shown in Table I, our method achieved an accuracy of 42.6%, outperforming the comparison methods listed in the table in terms of both mAP and mAR. This demonstrates that our method is highly generalizable and not dependent on a specific framework.

### C. Ablation studies

In this section, we conduct ablation experiments on DSAMD components to better understand the impact of different modules and configurations on the framework’s performance. The experimental setup is similar to that of previous experiments.

As shown in Table II, we use RetinaNet-ResNeXt101 as teacher and RetinaNet-Res50 as student. We explore two

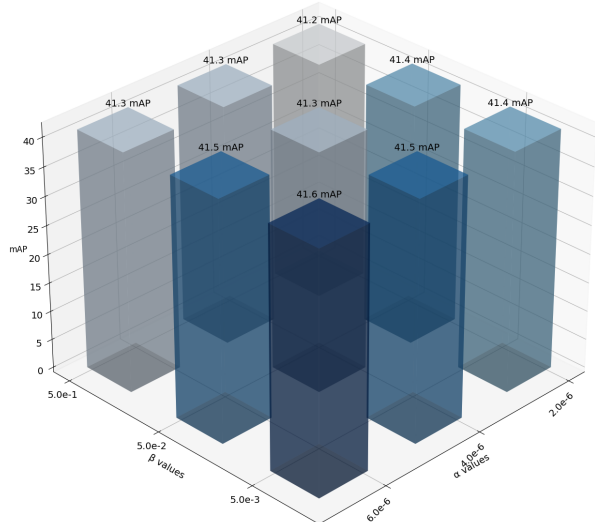


Fig. 4. Ablation studies of different  $\alpha$  and  $\beta$  on Retinanet framework.

primary modules in our DSAMD, namely the SA and AM. When only the SA component is applied, the model achieves the mAP of 41.5%. Interestingly, the inclusion of only the AM component results in a slightly lower mAP of 41.4%, indicating that SA has a more pronounced impact on improving performance. Finally, when both SA and AM are utilized together, the model achieves the best performance with the mAP of 41.6%. This demonstrates that the two components are complementary, and their combination effectively enhances the overall distillation performance. In Table III, we explore the impact of using Avg Pooling and Max Pooling in feature distillation, the experimental results show that using Max Pooling achieves the best improvement. In Table IV, we explore the impact of the Mask Weighting in logit distillation, the experimental results shows its effectiveness.

Furthermore, we conduct ablation experiments on different scales. As shown in Table V, using a single scale results in minor performance gains, while combining multiple scales progressively improves the mAP.

### D. Parameter Analysis

In our DSAMD method, the hyperparameters  $\alpha$  and  $\beta$  in (17) control the contributions of feature distillation and logit distillation. In our experiments, we used RetinaNet as the detection framework to discuss the impact of  $\alpha$  and  $\beta$ . As shown in Fig. 4, the best results are obtained when  $\alpha$  is set to  $5.0 \times 10^{-3}$  and  $\beta$  is set to  $6.0 \times 10^{-6}$ , yielding a maximum mAP of 41.6% and a maximum mAR of 57.7%.

## V. CONCLUSION

In this work, we investigate feature mask distillation under fine-grained division and propose a Fine-Grained Feature Maps Adaptive Masked Weights knowledge distillation method, DSAMD, for object detection. We enhance the student

model's ability to learn local features and boundary information through fine-grained division and max pooling, allowing it to learn more subtle features from the teacher network. Additionally, to improve global perception, we combine feature-based distillation with logit-based distillation by using feature-level masks as guidance. This hybrid approach helps logit localize information more effectively, facilitating the learning of more comprehensive global features. Extensive experiments demonstrate that DSAMD not only significantly improves the student model's performance but also outperforms other state-of-the-art distillation methods.

## REFERENCES

- [1] Tang, Q., Du, B. & Xu, Y. Self-supervised Learning Based on Max-tree Representation for Medical Image Segmentation. *2022 International Joint Conference On Neural Networks (IJCNN)*. pp. 1-6 (2022)
- [2] He, K., Gkioxari, G., Dollár, P. & Girshick, R. Mask r-cnn. *Proceedings Of The IEEE International Conference On Computer Vision*. pp. 2961-2969 (2017)
- [3] Lin, W., Li, Y., Ding, Y. & Zheng, H. Tree-structured Auxiliary Online Knowledge Distillation. *2022 International Joint Conference On Neural Networks (IJCNN)*. pp. 1-8 (2022)
- [4] Li, Z., Xu, P., Chang, X., Yang, L., Zhang, Y., Yao, L. & Chen, X. When object detection meets knowledge distillation: A survey. *IEEE Transactions On Pattern Analysis And Machine Intelligence*. **45**, 10555-10579 (2023)
- [5] Zhou, H., Song, L., Chen, J., Zhou, Y., Wang, G., Yuan, J. & Zhang, Q. Rethinking soft labels for knowledge distillation: A bias-variance tradeoff perspective. *ArXiv Preprint arXiv:2102.00650*. (2021)
- [6] Chen, D., Mei, J., Zhang, Y., Wang, C., Wang, Z., Feng, Y. & Chen, C. Cross-layer distillation with semantic calibration. *Proceedings Of The AAAI Conference On Artificial Intelligence*. **35**, 7028-7036 (2021)
- [7] Wang, X., Fu, T., Liao, S., Wang, S., Lei, Z. & Mei, T. Exclusivity-consistency regularized knowledge distillation for face recognition. *Computer Vision—ECCV 2020: 16th European Conference, Glasgow, UK, August 23–28, 2020, Proceedings, Part XXIV 16*. pp. 325-342 (2020)
- [8] Chen, P., Liu, S., Zhao, H. & Jia, J. Distilling knowledge via knowledge review. *Proceedings Of The IEEE/CVF Conference On Computer Vision And Pattern Recognition*. pp. 5008-5017 (2021)
- [9] Ross, T. & Dollár, G. Focal loss for dense object detection. *Proceedings Of The IEEE Conference On Computer Vision And Pattern Recognition*. pp. 2980-2988 (2017)
- [10] Zhang, L. & Ma, K. Structured knowledge distillation for accurate and efficient object detection. *IEEE Transactions On Pattern Analysis And Machine Intelligence*. (2023)
- [11] Yang, Z., Li, Z., Jiang, X., Gong, Y., Yuan, Z., Zhao, D. & Yuan, C. Focal and global knowledge distillation for detectors. *Proceedings Of The IEEE/CVF Conference On Computer Vision And Pattern Recognition*. pp. 4643-4652 (2022)
- [12] Yang, G., Tang, Y., Li, J., Xu, J. & Wan, X. Amd: Adaptive Masked distillation for object detection. *2023 International Joint Conference On Neural Networks (IJCNN)*. pp. 1-8 (2023)
- [13] Chen, G., Choi, W., Yu, X., Han, T. & Chandraker, M. Learning efficient object detection models with knowledge distillation. *Advances In Neural Information Processing Systems*. **30** (2017)
- [14] Yang, C., Ochal, M., Storkey, A. & Crowley, E. Prediction-guided distillation for dense object detection. *European Conference On Computer Vision*. pp. 123-138 (2022)
- [15] Cao, W., Zhang, Y., Gao, J., Cheng, A., Cheng, K. & Cheng, J. Pkd: General distillation framework for object detectors via pearson correlation coefficient. *Advances In Neural Information Processing Systems*. **35** pp. 15394-15406 (2022)
- [16] Zheng, Z., Ye, R., Wang, P., Ren, D., Zuo, W., Hou, Q. & Cheng, M. Localization distillation for dense object detection. *Proceedings Of The IEEE/CVF Conference On Computer Vision And Pattern Recognition*. pp. 9407-9416 (2022)
- [17] Zhao, B., Cui, Q., Song, R., Qiu, Y. & Liang, J. Decoupled knowledge distillation. *Proceedings Of The IEEE/CVF Conference On Computer Vision And Pattern Recognition*. pp. 11953-11962 (2022)
- [18] Lee, Y. & Wu, W. QMKD: A Two-Stage Approach to Enhance Multi-Teacher Knowledge Distillation. *2024 International Joint Conference On Neural Networks (IJCNN)*. pp. 1-7 (2024)
- [19] Ren, S. Faster r-cnn: Towards real-time object detection with region proposal networks. *ArXiv Preprint arXiv:1506.01497*. (2015)
- [20] Tian, Z., Shen, C., Chen, H. & He, T. FCOS: Fully Convolutional One-Stage Object Detection. *2019 IEEE/CVF International Conference On Computer Vision (ICCV)*. (2020)
- [21] Yang, Z., Liu, S., Hu, H., Wang, L. & Lin, S. Reppoints: Point set representation for object detection. *Proceedings Of The IEEE/CVF International Conference On Computer Vision*. pp. 9657-9666 (2019)
- [22] Duan, K., Bai, S., Xie, L., Qi, H., Huang, Q. & Tian, Q. Centernet: Keypoint triplets for object detection. *Proceedings Of The IEEE/CVF International Conference On Computer Vision*. pp. 6569-6578 (2019)
- [23] Carion, N., Massa, F., Synnaeve, G., Usunier, N., Kirillov, A. & Zagoruyko, S. End-to-end object detection with transformers. *European Conference On Computer Vision*. pp. 213-229 (2020)
- [24] Liu, Z., Lin, Y., Cao, Y., Hu, H., Wei, Y., Zhang, Z., Lin, S. & Guo, B. Swin transformer: Hierarchical vision transformer using shifted windows. *Proceedings Of The IEEE/CVF International Conference On Computer Vision*. pp. 10012-10022 (2021)
- [25] Zhu, X., Su, W., Lu, L., Li, B., Wang, X. & Dai, J. Deformable detr: Deformable transformers for end-to-end object detection. *ArXiv Preprint arXiv:2010.04159*. (2020)
- [26] Yang, G., Tang, Y., Wu, Z., Li, J., Xu, J. & Wan, X. DMKD: Improving Feature-Based Knowledge Distillation for Object Detection Via Dual Masking Augmentation. *ICASSP 2024-2024 IEEE International Conference On Acoustics, Speech And Signal Processing (ICASSP)*. pp. 3330-3334 (2024)
- [27] Lin, T., Maire, M., Belongie, S., Hays, J., Perona, P., Ramanan, D., Dollár, P. & Zitnick, C. Microsoft coco: Common objects in context. *Computer Vision—ECCV 2014: 13th European Conference, Zurich, Switzerland, September 6-12, 2014, Proceedings, Part V 13*. pp. 740-755 (2014)
- [28] Girshick, R. Fast r-cnn. *ArXiv Preprint arXiv:1504.08083*. (2015)
- [29] Everingham, M., Van Gool, L., Williams, C., Winn, J. & Zisserman, A. The pascal visual object classes (voc) challenge. *International Journal Of Computer Vision*. **88** pp. 303-338 (2010)
- [30] Shen, Z. & Xing, E. A fast knowledge distillation framework for visual recognition. *European Conference On Computer Vision*. pp. 673-690 (2022)
- [31] Huang, T., Zhang, Y., Zheng, M., You, S., Wang, F., Qian, C. & Xu, C. Knowledge diffusion for distillation. *Advances In Neural Information Processing Systems*. **36** pp. 65299-65316 (2023)
- [32] Yang, Z., Li, Z., Shao, M., Shi, D., Yuan, Z. & Yuan, C. Masked generative distillation. *European Conference On Computer Vision*. pp. 53-69 (2022)
- [33] Zhang, Y., Huang, T., Liu, J., Jiang, T., Cheng, K. & Zhang, S. FreeKD: Knowledge Distillation via Semantic Frequency Prompt. *Proceedings Of The IEEE/CVF Conference On Computer Vision And Pattern Recognition*. pp. 15931-15940 (2024)